https://doi.org/10.5194/egusphere-2026-2645
Preprint. Discussion started: 20 May 2026

Stable isotope signatures, concentrations, and potential supply of particulate organic carbon and nitrogen from summer sea ice in the Indian sector of the Southern Ocean

Keigo D. Takahashi[1,2], Ryosuke Makabe[3,4,5], Masayoshi Sano[3], Kazuki Nakata[6], Noriaki Kimura[7], Daiki Nomura[1,8], Michiyo Yamamoto-Kawai[5], Ryo Matsuda[9], Natsumi Nojiro[5], Masato Ito[10], Shintaro Takao[11], Naho Horimoto-Miyazaki[5], Aiko Tachibana[12], Norio Kurosawa[9], Takeshi Tamura[3,4], Mizuki Komatsu[13], Kay I. Ohshima[14], Kohei Mizobata[5], Shigeru Aoki[14], Masato Moteki[3,5]

[1]Faculty of Fisheries Sciences, Hokkaido University, Hakodate, 041-8611, Japan
[2]Japan Society for the Promotion of Science, Chiyoda, 102-0083, Japan
[3]National Institute of Polar Research, Tachikawa, 190-8518, Japan
[4]The Graduate University for Advanced Studies, SOKENDAI, Tachikawa, 190-8518, Japan
[5]Tokyo University of Marine Science and Technology, Minato, 108-8477, Japan
[6]Earth Observation Research Center, Japan Aerospace Exploration Agency, Tsukuba, 305-0047, Japan
[7]Faculty of Education, Kochi University, Kochi, 780-8520, Japan
[8]Arctic Research Center, Hokkaido University, Sapporo, 001-0021, Japan
[9]Faculty of Science and Engineering, Soka University, Hachioji, 192-8577, Japan
[10]Graduate School of Frontier Sciences, The University of Tokyo, Kashiwa, 277-8561, Japan
[11]National Institute for Environmental Studies, Tsukuba, 305-8506, Japan
[12]Japan Fisheries Research and Education Agency, Yokohama, 236-8648, Japan
[13]Japan Agency for Marine-Earth Science and Technology, Yokohama, 236-0001, Japan
[14]Institute of Low Temperature Science, Hokkaido University, Sapporo, 060-0819, Japan

Correspondence to: Keigo D. Takahashi (keigo.d.takahashi@gmail.com)

Abstract. The primary production and zooplankton life cycles in the Southern Ocean synchronize with seasonal sea ice melting, during which particulate organic carbon (POC) and nitrogen (PN), including ice algae, are supplied from sea ice into the water column. To understand carbon flow through food webs in this productive marginal ice zones, it is necessary to determine the quantity and quality of organic carbon and nitrogen in sea ice. However, knowledge regarding brash sea ice is scarce, even though it is the predominant form at the Antarctic ice edge. In this study, 102 sea-ice samples were collected from the Indian sector (20–160°E) during summer to clarify variations in isotopic baselines and the potential contribution of sea ice-derived carbon and nitrogen to the water column. The $\delta^{13}C$ and $\delta^{15}N$ values of sea-ice particulate matter were −24.5±3.2‰ and +1.6±2.2‰ (mean±standard deviation), respectively, showing greater variability compared to those in seawater (−28.8±1.0‰ for $\delta^{13}C$ and −0.5±1.4‰ for $\delta^{15}N$). We identified correlations of $\delta^{13}C$ and $\delta^{15}N$ with organic matter and nutrient concentrations and their ratios (e.g., silicate:nitrate), indicating that nutrient consumption and organic matter decomposition influenced those isotopic characteristics in sea ice. Using freshwater flux from sea ice melt and the measured sea-ice POC concentrations, this supply was estimated to be 4.6±0.3 Tg C $year^{-1}$, equivalent to >14% of primary production

https://doi.org/10.5194/egusphere-2026-2645
Preprint. Discussion started: 20 May 2026

in the marginal ice zone of the studied region. These results suggest that the carbon supply from sea ice is a crucial factor supporting ecosystems in the seasonal sea ice zone.

1 Introduction

The Southern Ocean is known as a carbon sink, absorbing 43% of the anthropogenic carbon dioxide from the atmosphere (Frölicher et al., 2015). This carbon uptake is driven not only by the high solubility of carbon dioxide in cold water and the formation of deep water, but also by the atmospheric-oceanic imbalance resulting from phytoplankton photosynthesis and the drawdown of dissolved inorganic carbon. In the Southern Ocean, approximately 90% of the organic matter produced by phytoplankton is consumed by herbivorous zooplankton, whereas only 10% is consumed by phytodetritus (Moreau et al., 2020). Because organic matter leads to long-term carbon sequestration by sinking below the winter thermocline as aggregates or zooplankton fecal pellets, understanding ecosystem structures, such as predator-prey relationships and trophic levels, is essential for understanding carbon flow.

A notable feature of the Southern Ocean is its vast seasonal sea ice zone (SIZ), where biological activity is closely related to sea ice expansion and retreat (Ardyna et al., 2017). Ice-edge phytoplankton blooms can occur during sea ice melting (Wilson et al., 1987). Although it is a temporal phenomenon that generally terminates within two weeks, it accounts for more than 10% of primary production south of 50°S (Arrigo et al., 2008). Primary consumers (such as copepods and salps), which are crucial for driving biological pumps and sequestering organic carbon into the deep ocean, have life cycles that rely on carbon dynamics following ice melting. Long-term variability in sea ice concentration and extent (Eayrs et al., 2021) is believed to affect the succession of these primary consumer communities. However, ice-edge blooms occur in only approximately 20% of the area (Fitch and Moore, 2007) because of large variations in iron supply, water-column stratification, and the released ice algae, which serve as a seeding population. Although significant heterogeneity in phytoplankton biomass (chlorophyll *a* [Chl *a*] concentration) has been observed, zooplankton abundance is distributed more ubiquitously (Takahashi et al., 2011). Hence, understanding how zooplankton consume particulate organic matter (POM) contributes to our understanding of the carbon cycle driven by biological pumps in the Southern Ocean.

Studies on herbivorous zooplankton in the east Antarctic SIZ have shown that their development depends more on the timing of sea ice retreat than on the occurrence or magnitude of ice-edge blooms (Makabe et al., 2017; Tachibana et al., 2023; Sugioka et al., 2021); this suggests that they may depend on sea ice organic matter, as well as that associated with ice-edge blooms. Primary consumers in seasonal sea ice regions, such as krill and copepods, are mostly filter feeders, suggesting that non-algal organic particles, such as detritus, could serve as food sources. Reviews by Dalman et al. (2025) summarized high particulate organic carbon (POC) concentrations (>1,000 μg L^{-1}) and POC:Chl *a* ratios (>1,000) in the upper summer sea-ice cores. The release of POC during sea ice melt could provide an important food source for zooplankton communities for the production associated with ice-edge blooms. Therefore, to understand the supply of matter and organisms from sea ice to the

https://doi.org/10.5194/egusphere-2026-2645
Preprint. Discussion started: 20 May 2026

water column associated with large-scale sea ice melt at the ice edge, it is necessary to collect melting sea ice in the summer in the Southern Ocean and accumulate data.

In addition to POC and particulate nitrogen (PN) concentrations, insights into the quality of POM in sea ice, specifically its stable isotope ratios, are crucial for understanding ecosystem structure. The $\delta^{13}C$ values of POM are used to estimate prey resources, while $\delta^{15}N$ is used to estimate trophic levels. The position of each zooplankton within the food web and its prey resources were estimated (Schmidt et al., 2003; Liu and Zhou, 2025). Sea-ice $\delta^{15}N$ varies significantly, with values ranging from −4.9‰ to +6.0‰ used as the baseline for ice algae (Mincks et al., 2008; Jia et al., 2016). However, the maximum values reported is +41‰ (Rau et al., 1991). As Wada et al. (1987) determined the zooplankton trophic level as $\delta^{15}N_{Zooplankton} = 3.3$ (Trophic level−1) + $\delta^{15}N_{Baseline}$, variability in $\delta^{15}N_{Baseline}$ (algae) values could significantly affect estimates of food web structures. Similarly, $\delta^{13}C$ ranges from −28‰ to −10‰ in sea ice (Munro et al., 2010; Wing et al., 2018), which has greater variability than the $\delta^{13}C$ of POM in seawater within the SIZ (approximately −30‰ to −28‰, Rau et al., 1991). These studies suggest that understanding the isotopic characteristics of POM in sea ice will contribute to the understanding of carbon pathways in planktonic food webs of the SIZ.

To date, much of the POM data have been obtained from sea-ice core samples collected during spring, when fast ice and pack ice floes are well established to land on ice. Consequently, knowledge of POM concentrations and their isotopic ratios in more melted sea ice (such as brash ice) or at lower latitudes (offshore) remains limited to certain areas, such as off Cape Darnley (Takahashi et al., 2023). Brash sea ice is fragmented and melted into smaller pieces (generally <2 m), possessing distinct biogeochemical compositions and physical properties compared to ice floes (Takahashi et al., 2022; Nomura et al., 2023). Furthermore, because of their high surface-area-to-volume ratio, they are thought to melt rapidly from spring to summer, influencing dissolved and particulate biogeochemical components in the ocean surface layer (Takahashi et al., 2022; Nomura et al., 2023; Akino et al., 2024). For example, organisms within broken ice receive higher irradiance than intact floes. Moreover, a high brine volume fraction (Nomura et al., 2023) and surface area-to-volume ratio are thought to enable gas exchange (e.g., carbon dioxide) between brash ice and the atmosphere. Considering that light intensity and dissolved inorganic carbon concentration influence the POC isotope composition of diatoms (Thompson and Calvert, 1994; Kennedy et al., 2002), such environments may yield $\delta^{13}C$ values distinct from those reported from ice floes in previous studies.

We collected sea ice from various locations in the Indian sector of the Southern Ocean (20°–160°E) from January 2016 to early March 2020. The objectives of this study were to determine the quantity and quality of POM within drift ice in the region and to clarify the factors influencing the CN isotopic characteristics by analyzing other parameters, such as Chl *a* and nutrient concentrations. Furthermore, we discuss the potential of sea ice melt as a carbon source during the summer. The contribution of algae-derived carbon was estimated using the algal POC:Chl *a* ratio reported in prior microscopic observations of sea ice.

https://doi.org/10.5194/egusphere-2026-2645
Preprint. Discussion started: 20 May 2026

2.1 Sea ice and seawater sampling

Sea ice samples were collected from 24 stations during nine voyages conducted between January 2016 and March 2020 (Fig. 1; Table 1). The collected sea ice was brash ice (drift ice <2 m in diameter) originating from first-year ice/older ice (FYI/OI) and newly formed ice (pancake ice and nilas). On the training vessel *Umitaka-maru* (Tokyo University of Marine Science and Technology, UM15-08, UM16-08, UM18-08, UM19-08), drift ice was scooped up by the crane using a plankton net frame covered with cloth (Takahashi et al., 2022). On the icebreaker *Shirase* (JARE57, JARE61) and the research vessel *Hakuho-maru* (KH19-01, KH20-1), samples were collected manually and randomly using steel baskets and fishing nets (Takahashi et al., 2023; 2025), respectively. The collected sea ice was immediately packed into polyethylene bags and stored in the dark at −20°C until analysis. Seawater was sampled almost twice daily in January 2019 (UM18-08 cruise) using a continuous underway pump (5 m depth) aboard *Umitaka-maru*. A total of 1.0 to 2.3 L of seawater was filtered through the pre-combusted Whatman GF/F filters (450°C, 4 h). The filters were packed into cryovials and transported to the laboratory in liquid nitrogen.

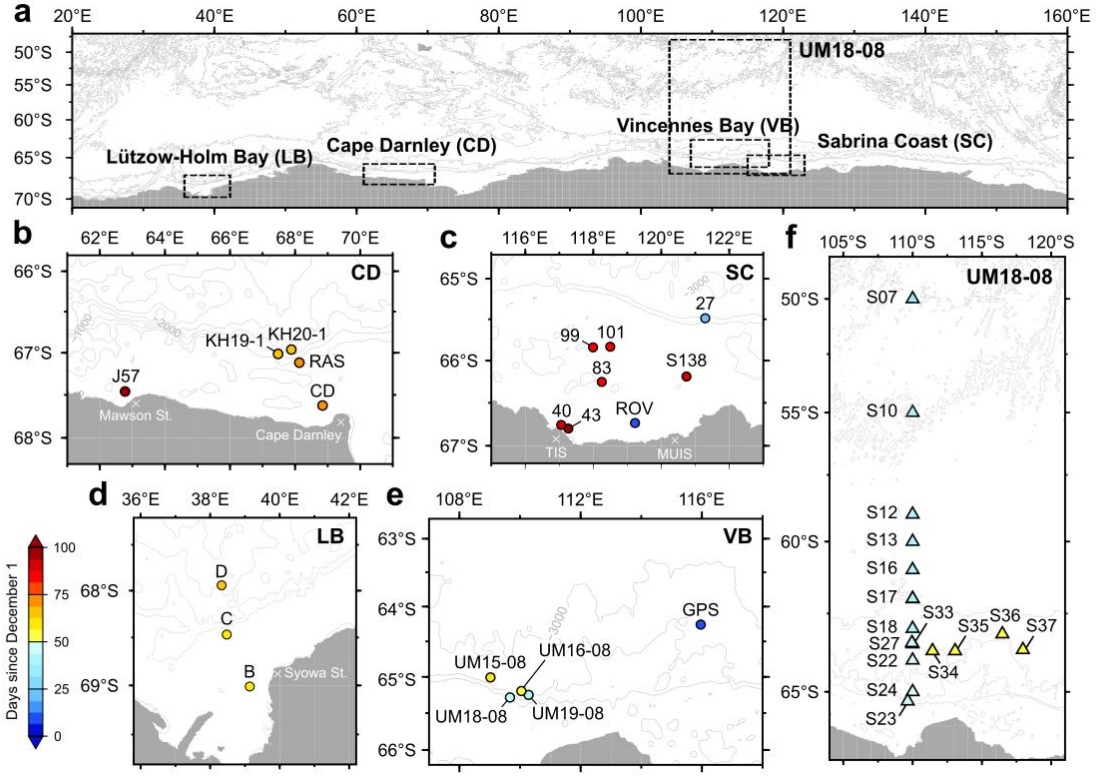

Figure 1: Study area of the Indian sector of the Southern Ocean (a) and the sampling stations of sea ice in each region (b–e). CD: Off the Cape Darnley (b), SC: Sabrina Coast (c), LB: Lützow-Holm Bay, VB (d): Offshore region around the Vincennes Bay (e). Circles and triangles indicate sampling sites of sea ice and surface seawater, respectively.

https://doi.org/10.5194/egusphere-2026-2645
Preprint. Discussion started: 20 May 2026

Table 1: Sampling date and physical and biological properties of sea ice at each station. The en dash (–) indicates no data. Means and standard deviations are shown, except for stations where only two sea ice samples were collected. The DSF indicates the number of days elapsed since sea ice formation, which was estimated using remote sensing. Newly formed ice stations and stations with no valid ice data (e.g., low sea ice concentration) were excluded from the DSF analysis. LB: Lützow-Holm Bay; CD: Cape Darnley; VB: Vincennes Bay; SC: Sabrina Coast.

Region	Station	Date	Salinity	Chl *a* (μg L^{-1})	POC (μg L^{-1})	PN (μg L^{-1})	$\delta^{13}C$ (‰)	$\delta^{15}N$ (‰)	DSF (days)	*n*
LB	B	Jan. 29, 2020	2.1	0.8	594.9	34.6	−24.6	0.1	561	2
LB	C	Jan. 31, 2020	7.3±3.0	43.1±30.2	1795.2±582.7	188.2±71.1	−21.1±0.6	0.6±1.0	299	3
LB	D	Feb. 2, 2020	6.1±3.4	11.1±3.8	2726.8±1331.6	287.8±128.9	−23.0±0.8	0.2±0.5	320	3
CD	J57[a]	Mar. 6, 2016	14.5	1.9	534.8	44.9	−24.6	–	–	2
CD	KH19-1	Feb. 2, 2020	3.6±1.4	75.7±66.4	3017.5±1343.3	389.2±226.3	−24.2±1.6	2.5±3.5	–	5
CD	KH20-1	Feb. 3, 2020	1.0±0.6	0.1±0.1	1219.3±493.5	64.8±27.3	−26.3±0.4	3.4±1.0	308	3
CD	CD	Feb. 10, 2020	6.4±3.0	12.6±16.0	1621.2±661.0	155.5±115.2	−26.2±1.7	3.0±3.8	310	3
CD	RAS	Feb. 9, 2020	3.3	2.5	769.2	62.0	−25.9	0.6	528	2
VB	UM15-08	Jan. 27, 2016	2.2±1.6	9.5±19.2	1784.6±2235.4	174.4±256.1	−24.5±2.2	–	558	9
VB	UM16-08	Jan. 11, 2017	2.5±0.8	4.2±4.4	767.8±227.0	69.9±26.8	−24.8±0.7	1.8±4.0	555	10
VB	UM18-08	Jan. 16, 2019	1.9±1.5	4.1±5.2	671.1±261.0	66.9±34.4	−27.0±3.6	0.6±1.1	489	12
VB	UM19-08	Jan. 22, 2020	3.4±0.7	28.0±19.4	1718.9±680.3	130.3±28.3	−19.7±4.2	2.8±1.2	330	10
VB	GPS	Dec. 9, 2019	5.4±1.0	3.1±3.6	727.6±531.0	56.6±49.5	−26.2±2.0	0.8±1.7	310	10
SC	16	Dec. 17, 2019	9.9±1.3	37.0±6.9	1871.0±105.9	214.7±38.3	−22.4±0.8	2.7±0.2	203	3
SC	ROV	Dec. 12, 2019	4.8±1.8	5.7±4.3	476.2±259.7	53.6±34.3	−24.0±1.4	2.1±1.0	–	3
SC	27	Dec. 20, 2019	7.1±1.3	13.1±7.9	859.2±610.1	79.8±54.4	−24.8±1.4	1.1±0.5	314	3
SC	83	Feb. 22, 2020	3.0±1.3	14.0±13.9	1119.6±612.2	84.7±54.9	−25.6±1.6	−0.3±1.4	386	5
SC	99	Feb. 25, 2020	4.0	47.5	2557.9	297.9	−23.7	2.7	534	2
SC	101	Feb. 25, 2020	4.9±2.0	33.3±31.3	1894.6±1164.6	219.9±185.2	−22.9±1.5	2.8±1.9	368	3

https://doi.org/10.5194/egusphere-2026-2645
Preprint. Discussion started: 20 May 2026

SC	40	Feb. 27, 2020	4.9	5.8	1825.9	119.1	−24.8	2.3	560	2
SC	43[a]	Feb. 27, 2020	15.9±2.2	3.2±0.8	664.3±192.1	40.7±11.5	−28.1±0.6	0.5±2.1	–	3
SC	S138[a]	Mar. 5, 2020	9.8±0.4	0.2±0.0	997.6±349.4	32.1±9.3	−26.9±0.8	0.1±0.6	–	4

[a]Stations of newly formed ice.

2.2 Sea ice melting and subsampling procedures

After measuring the total weight of sea ice, the ice blocks were roughly crushed with an ice pick to homogenize them, then randomly divided into 200–800 g portions (excluding UM15-08 and UM16-08). This ice was melted in 9 times the volume of 0.2 µm-filtered seawater at 4°C in the dark, and the meltwater was filtered through Whatman GF/F filters to measure Chl *a* concentration. The remaining sea ice was then melted in polyethylene bags at room temperature in the dark (Roukaerts et al., 2019). Meltwater was filtered through pre-combusted Whatman GF/F filters and stored in a deep freezer. The subsequent drying and fumigation followed the procedure for seawater POM filters. Salinity was measured from a portion of the meltwater collected for nutrient analysis, which was then stored in a deep freezer (−80°C). Sea ice volume was calculated from salinity, meltwater temperature (+4°C), and weight of sea ice.

2.3 Chl *a* concentration

Meltwater from sea ice samples and surface seawater was filtered through Whatman GF/F filters. The pigments were extracted with *N*,*N*-Dimethylformamide for at least 24 h (Suzuki and Ishimaru, 1994) and Chl *a* concentrations were measured using a pre-calibrated fluorometer (Welschmeyer, 1994). For sea-ice samples from Sts. UM15-08 and UM16-08, all Chl *a* samples were collected from meltwater without adding filtered seawater. However, the effect of osmotic changes on bulk Chl *a* concentration is considered insignificant (Dieckmann et al., 1988; Meiners et al., 2012).

2.4 POC and PN concentrations and stable isotope composition

The POM filters were dried at 60°C for 24 h, fumed with 1 mol L^{-1} hydrochloric acid (HCl) to remove particulate inorganic carbon, and stored in a desiccator. The filter samples were packed into tin capsules and analyzed for POC and PN concentrations and stable isotope ratios ($\delta^{13}C$, $\delta^{15}N$) using the isotope ratio mass spectrometry (Flash 2000-ConfoIV-DeltaV advantage, Thermo Scientific, USA; Europa PPZ GEO 20-20). $\delta^{13}C$ and $\delta^{15}N$ were calculated using the following equations based on the differential ratios relative to standard materials.

$$\delta^{x} = \left(\left[\frac{R_{sample}}{R_{standard}}\right] - 1\right) \times 10^{3} \quad (1)$$

where x is either ^{13}C or ^{15}N and R_{sample} and $R_{standard}$ are the isotope ratios ($^{13}C/^{12}C$ and $^{15}N/^{14}N$) of the samples and standard materials, respectively.

https://doi.org/10.5194/egusphere-2026-2645
Preprint. Discussion started: 20 May 2026

2.5 Nutrient concentrations

Nutrient concentrations (NO_3^-, PO_4^{3-} $Si(OH)_4$) in sea ice collected by *Umitaka-maru* from 2016 to 2019 (UM15-08, UM16-08, UM18-08) and sea ice collected by *Shirase* in 2016–2017 and 2018–2019 (JARE57, JARE59) were measured using the methods described in Shimada et al. (2020). Sea ice from the *Hakuho-maru* voyages (KH19-01 and KH20-01) and the 2019–2020 *Shirase* voyage (JARE61) were measured in accordance with JGOFS (1994). For UM18-08, JARE61, and KH19-01 sea ice nutrients, some data are cited from the previous studies (Takahashi et al., 2022; 2023; 2025, Nomura et al., 2023).

To visually analyze the consumption and remineralization of each nutrient (NO_3^-, PO_4^{3-}, $Si(OH)_4$) since sea ice formation, comparisons with the Theoretical Dilution Line (TDL) were conducted. The mean nutrient concentrations and salinity (34.3) from the summer minimum temperature layer, measured in the eastern Antarctic SIZ, were cited from Nomura et al. (2023) as initial (autumn to winter) seawater values. Bulk sea ice nutrient concentrations depend on brine discharge, sea ice freezing and melting, and snow accumulation, which dilute nutrients. To isolate the effects of biological accumulation and consumption processes on other components (e.g., POC concentration), the salinity-normalized nutrient concentrations ($*NO_3^-$, $*PO_4^{3-}$, $*Si(OH)_4$) were calculated (Fripiat et al., 2017), which were expressed as:

$$* C = \frac{C \times 34.3}{S} \quad (2)$$

Here, C represents the bulk nutrient concentration, and S represents the salinity of sea ice.

2.6 Contribution of algal carbon to POC

The conversion of algae in sea ice to carbon was estimated from the POC:Chl *a* ratio reported in previous studies (Becquevort et al., 2009; Meiners et al., 2011; Takahashi et al., 2023). The POC:Chl *a* ratio for isolated cultured strains has been reported to be 25–96 for the Antarctic diatom *Fragilariopsis cylindrus* and 41–284 for the haptophyte *Phaeocystis antarctica* (Arrigo et al., 2010). However, these values are highly dependent on culture light conditions and are unlikely to reflect sea ice in natural environments inhabited by diverse communities. Therefore, this study used the ratio of ice-algal carbon (IAC) to chlorophyll *a* concentration, estimated from field observations. Previously, the IAC:Chl *a* ratios for Antarctic ice algae (based on linear regression) were reported to range from 32.5 to 91.7 (Becquevort et al., 2009; Meiners et al., 2011; Takahashi et al., 2023). We calculated ice-algal carbon content (POC_{algae}, μg C L^{-1}) by multiplying sea-ice Chl *a* concentration by the mean IAC:Chl *a* ratio (54.4±26.5).

$$POC_{algae} = Chl\ a \times F \quad (3)$$

Additionally, by dividing POC_{algae} by the POC concentration, we estimated the proportion of algae-derived carbon (%).

2.7 Sea-ice back trajectory and ice production based on remote sensing

To reconstruct the trajectories of sea ice after its formation, we estimated sea ice motion based on satellite observations (Kimura, 2004). Specifically, backward trajectories of virtual particles were calculated using daily gridded sea ice drift velocity data with a spatial resolution of 60 km. Each particle was advected backward in time following the ice motion field.

https://doi.org/10.5194/egusphere-2026-2645
Preprint. Discussion started: 20 May 2026

When a particle reached a grid cell where no sea ice was present, that location was regarded as the point of initial sea ice formation for the particle (Corkill et al., 2023, etc.). However, it remains unclear whether sea ice was formed at this specific point. In this study, we estimated daily sea-ice production along the sea-ice trajectory to better identify its origin. First, the thermal ice thickness was estimated following Nakata et al. (2019) using microwave data from AMSR2 on board GCOM-W. The daily sea-ice production (m day^{-1}, 6.25 km grid resolution) was calculated by the heat budget analyses (Nakata et al., 2021) using ECMWF ERA5 reanalysis products (Hersbach et al., 2018, 2020) and the estimated thermal ice thickness. We extracted sea ice production only along the trajectory. The first date of sea-ice production is defined as the first time sea ice was produced (>0.00 m day^{-1}) across all available trajectory data, and the elapsed days from sea-ice formation to ice sampling (DSF) are calculated.

2.8 Sea ice melt thickness and POC flux from sea ice

To estimate POC and algae-derived POC (Section 2.6.) supply from sea ice, we determined the average POC and Chl *a* concentrations within sea ice during the melt season. Because this study randomly sampled broken ice, it included sea ice of various sizes. To estimate the POC concentration in meltwater when these sea-ice samples melt, it is necessary to account for differences in ice piece size (melt volume). Using the POC concentration of all sea ice (excluding newly formed ice) and the volume calculated from sea ice weight, we calculated the volume-weighted mean (VWM) POC and Chl *a* concentrations, following Takahashi et al. (2022).

$$POC_{VWM} = \frac{\sum_{i=1}^{n}(a_i \times b_i)}{\sum_{i=1}^{n} b_i} \quad (4)$$

$$Chl_{VWM} = \frac{\sum_{i=1}^{n}(c_i \times b_i)}{\sum_{i=1}^{n} b_i} \quad (5)$$

Here, n is the total number of ice samples, and i indexes each ice sample. a_i and c_i represent the concentrations of POC or Chl *a* (μg L^{-1}), respectively, in the sea-ice sample number i, and b_i is the volume (L) of the sample. Chl_{VWM} was converted to algal-derived POC by multiplying it by an IAC:Chl *a* ratio of 54.4±26.5 (Section 2.6).

We adopted the VWM method to determine POC content in meltwater in order to avoid biases when a mathematical mean was used. In extreme case, release of POC into seawater from quite small sea ice (sample volume: 0.4 L) with high POC concentration (5,000 μg L^{-1}) is equivalent to that from larger ice (10 L) with low POC concentration (200 μg L^{-1}) if both of them were melted (POC_{VWM}: 2,000 μg L^{-1}). In this situation, using a simple mean value (2,600 μg L^{-1}) would make the contribution of POC concentration in larger-sized sea ice minor and the other way around. Although the VWM method cannot calculate the variance SD, it can correct for such bias when dealing with the samples with different size or concentrations.

https://doi.org/10.5194/egusphere-2026-2645
Preprint. Discussion started: 20 May 2026

Next, we estimated the freshwater flux from sea ice melt (unit: sea ice melt thickness [m]). The freshwater flux was calculated using climate values from Komatsu et al. (2025) and averaged over the study area (20–160°E). The sea ice meltwater flux was multiplied by the POC_{VWM} concentration in sea ice to estimate the POC flux from sea ice to the water column per unit area (mg C m^{-2} $year^{-1}$). To estimate the contribution of the POC flux from sea ice to primary production in the water column, we cited the means (±standard deviation: SD) of SIZ area (difference of ice extent in September and February) during 1979–2019 (Parkinson, 2019) and the primary production for the summer MIZ and MIZ shelves during 1997–2006 (Arrigo et al., 2008) in the Indian sector of the Southern Ocean. The SD for the contribution of sea-ice POC to the production in seawater was calculated by propagation of error using SD of POC input and primary production in the MIZ.

2.9 Statistical analyses

To identify factors influencing variations in sea-ice POC, PN concentrations, and POM stable isotope ratios ($\delta^{13}C$, $\delta^{15}N$), we investigated correlations between these data and salinity, Chl *a*, salinity-normalized nutrient concentrations, the $Si(OH)_4$:NO_3^- ratio, the NO_3^-:PO_4^{3-} ratio, and DSF. For each dataset, Q-Q plots were first used to assess whether parametric tests were appropriate. Since linear regression could not be applied to some parameter sets, a nonparametric Spearman's rank correlation test was used for all correlations, except the POC:PN ratio, to assess the presence of significant relationships and to calculate correlation coefficients. For POC, PN concentrations, $\delta^{13}C$, and $\delta^{15}N$ in the four areas (LB, CD, VB, SC; Fig. 1), the datasets were non-normal according to the Kolmogorov–Smirnov test. Therefore, the Kruskal-Wallis test and Steel-Dwass tests were used to confirm differences in medians across areas. All statistical analyses were performed using the R software (https://www.r-project.org/).

3 Results

3.1 Characteristics of salinity, macronutrient, and POM concentrations in sea ice and seawater

The POC concentrations in sea ice ranged 246.1–6365.3 µg L^{-1} and showed a linear relationship with PN (14.4–725.4 µg L^{-1}) (Fig. 2). The POC:PN ratio (g:g) ranged from 4.5 to 41.9, with an average of 13.4, and the ratio obtained from linear regression was 7.6. Sea-ice POM $\delta^{13}C$ and $\delta^{15}N$ ranged from −35.1‰ to −3.1‰ and −3.8‰ to +11.1‰, respectively, showing a significant positive correlation with each other (Spearman's rank test, r=0.24, p<0.01), although the correlation coefficient was low.

The POC and PN concentrations in surface seawater showed lower values and smaller variations compared to sea ice ranging 79.7–302.5 µg L^{-1} and 13.9–64.3 µg L^{-1}, respectively. Chl *a* concentration was also consistently low (0.2–1.8 µg L^{-1}) except the maximum found at St. S35. Seawater POM $\delta^{13}C$ and $\delta^{15}N$ ranged from −30.9‰ to −27.0‰ and −3.1‰ to +1.5‰, respectively and no relationships were observed between them.

https://doi.org/10.5194/egusphere-2026-2645
Preprint. Discussion started: 20 May 2026

Sea-ice salinity ranged from 0.3 to 10.6 in FYI/OI-derived sea ice and from 9.4 to 18.4 in newly formed ice. NO_3^-, PO_4^{3-}, and $Si(OH)_4$ concentrations in sea ice were 0.5–15.9 µmol L^{-1}, 0.0–8.0 µmol L^{-1}, and 0.0–21.3 µmol L^{-1}, respectively (Fig. 2). All nutrients showed a positive correlation with sea ice salinity, with the highest concentrations observed in the new ice from the SC. Compared to seawater (winter TDL), plots for NO_3^-, PO_4^{3-}, and $Si(OH)_4$ fell below the TDL in 43%, 7%, and 93% of samples, respectively. The proportion of sea ice samples falling below the TDL showed no significant regional variation for NO_3^-.

https://doi.org/10.5194/egusphere-2026-2645
Preprint. Discussion started: 20 May 2026

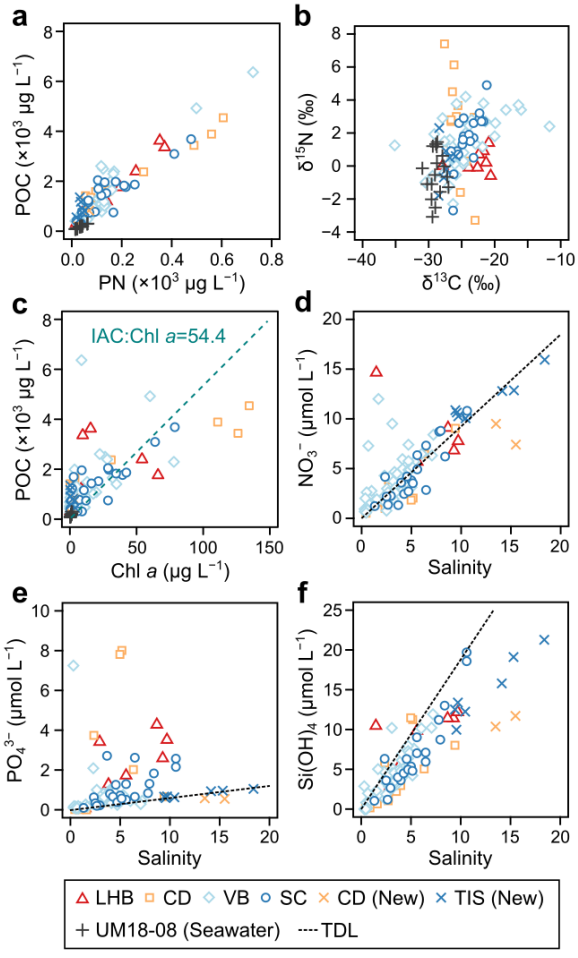

Figure 2: Relationships between concentrations or isotopic ratios of particulate organic carbon and nitrogen and Chl *a* and in sea ice and seawater (a–c). Sea-ice salinity and macronutrient concentrations (d–f). TDL denotes theoretical dilution line. LB: Lützow-Holm Bay; CD: Cape Darnley; VB: Vincennes Bay; SC: Sabrina Coast.

The tracked trajectory of the sea ice revealed that much of it drifted from the east (Supplementary Figs. S1–S3). The number of days since the sea ice formation (DSF) ranged from 203 to 581 days (Table 1). Even within the same sea area (LB, CD, VB, and SC), the DSF varied significantly, ranging from sea ice less than 1-year old to ice likely to be second-year ice (DSF >500 days).

3.2 Regional variations of Chl *a* and POM concentrations and isotope signatures

To examine the regional variations and differences between sea ice types (FYI/OI and newly formed ice) for each parameter, the values were plotted for the four regions (Fig. 3). The sea ice salinity of the FYI/OI from all stations was significantly

https://doi.org/10.5194/egusphere-2026-2645
Preprint. Discussion started: 20 May 2026

lower than that of the newly formed ice. Significant salinity differences were observed between the VB (mean 3.0) and SC (mean 5.4) (Steel-Dwass test, $p<0.05$). Chl *a* concentrations in FYI/OI ranged 0.01–134 μg L^{-1}, showing higher average concentrations compared to newly formed ice (0.2–4.0 μg L^{-1}). Except for CD, FYI/OI had significantly higher Chl *a* concentrations than the newly formed ice (Steel-Dwass test, $p<0.05$).

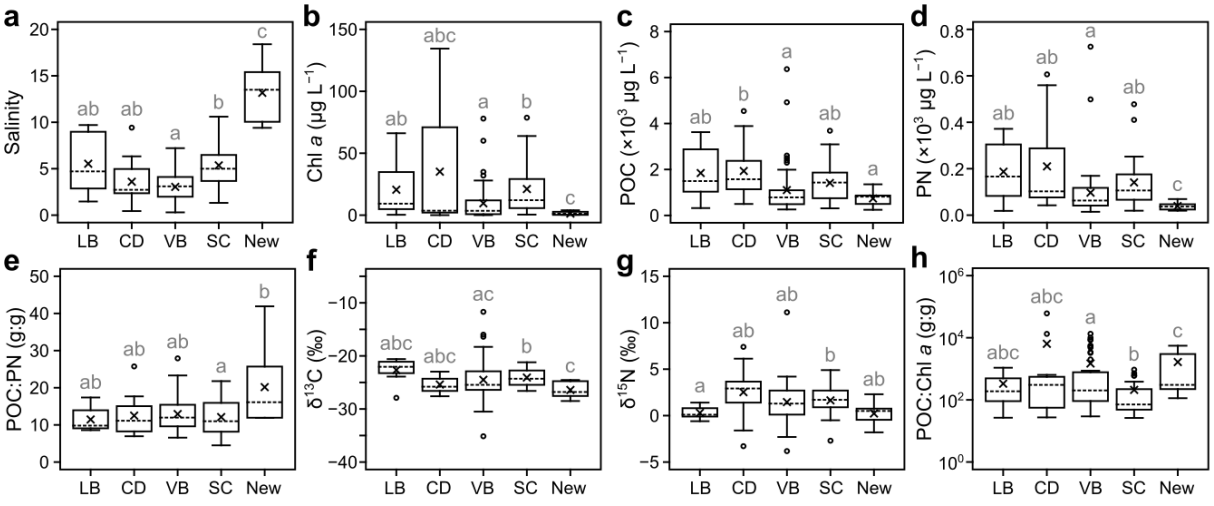

Figure 3: Regional or ice-type (FYI/OI brash ice v.s. newly formed ice) differences in salinity (a), Chl *a* (b), POC (c), PN (d) concentrations and POC:PN ratios (e), stable isotopes of POC (f) and PN (g), and POC:Chl *a* ratios (h) in sea ice. X and horizontal dotted lines indicate the mean and median, respectively. LB: Lützow-Holm Bay; CD: Cape Darnley; VB: Vincennes Bay; SC: Sabrina Coast.

Similar to Chl *a*, POC concentrations of FYI/OI were higher than the average value for newly formed ice (738.3 μg L^{-1}), but significant differences in POC concentration were only observed between those of CD and VB, and between CD and newly formed ice. Unlike POC, PN concentrations showed no significant differences between FYI/OI, whereas newly formed ice was significantly lower than VB, CD, and SC. The POC:PN ratio for FYI/OI ranged from 4.5 to 12.6, showing lower values and less variation compared to new ice (11.9–41.9). However, significant differences were observed only between the SC and newly formed ice (Steel-Dwass test, $p<0.05$).

The mean (±SD) $\delta^{13}C$ and $\delta^{15}N$ values for sea ice excluding newly formed ice were −24.4±3.2‰ and 1.6±2.2‰, respectively (−24.6±3.2‰ and 1.5±2.2‰ for all sea ice). The $\delta^{13}C$ of newly formed ice was significantly lower than that of SC, but among FYI/OI samples, a significant difference was observed only between VB and SC. In contrast, for $\delta^{15}N$, no significant differences were found between regions or newly formed ice, except that SC was significantly higher than LB. The POC:Chl

https://doi.org/10.5194/egusphere-2026-2645
Preprint. Discussion started: 20 May 2026

a ratio showed significant differences among the VB, SC, and newly formed ice, with the highest average value observed in the newly formed ice.

3.3 Monthly variations in physical properties and biogeochemical components of sea ice

To clarify whether the physical parameters and particulate matter within sea ice varied across sampling periods, the above components were plotted separately for December, January, and February (Fig. 4), excluding newly formed ice. The sea ice salinity showed significant differences between December and February. The average salinity peaked in December (6.3), declined to 2.8 in January, and increased slightly to 4.0 in February. The Chl *a* concentration in the sea ice increased from December to February. Although the average value in February was more than 2.1 times higher than that in the preceding months, no significant monthly differences were observed (Kruskal-Wallis test, p=0.26). Monthly POC concentrations showed a trend similar to that of Chl *a*, with both significantly higher in February than in other months. The PN concentration also tended to increase in February, but a significant difference was only observed between December and February. However, the rate of increase from January to February was 1.6 times for POC and 1.8 times for PN, which was more moderate than the increase in Chl *a* concentration. POC:PN and POC:Chl *a* ratios, $\delta^{13}C$, and $\delta^{15}N$ showed some monthly variations, but no significant differences were discerned (Kruskal-Wallis test, p>0.29).

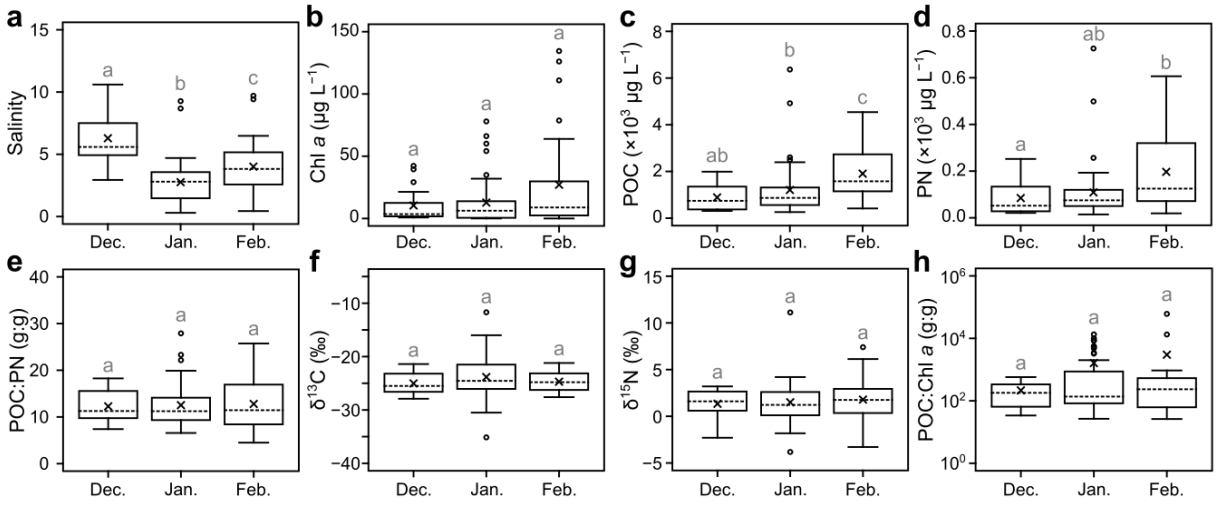

Figure 4: Monthly variations of salinity (a), Chl *a* (b), POC (c), PN (d) concentrations and POC:PN ratios (e), stable isotopes of POC (f) and PN (g), and POC:Chl *a* ratios (h) in sea ice. X and horizontal dotted lines indicate the mean and median, respectively.

https://doi.org/10.5194/egusphere-2026-2645
Preprint. Discussion started: 20 May 2026

3.4 Inter-relationships between biogeochemical components in sea ice and seawater

To identify the factors affecting the sea ice POC and PN concentrations and their respective isotope ratios, we investigated their correlations with other physical and biogeochemical parameters (Fig. 5). Sea-ice POC and PN concentrations showed positive correlations with Chl *a* and $*PO_4^{3-}$ concentrations and $Si(OH)_4:NO_3^-$ (Spearman's rank test, $r>0.30$, $p<0.05$), while they correlated negatively with $*NO_3^-$ and DSF ($r<-0.20$, $p<0.05$, Fig. 5a). Chl *a* concentration showed similar results to POC and PN regarding Chl *a* and $*PO_4^{3-}$, but it also exhibited a weak positive correlation with salinity (Spearman's rank test, $r=0.35$, $p<0.05$). DSF showed negative correlations with Chl *a* concentration and salinity, similar to POC and PN, but a positive correlation was also observed between POC:Chl *a* ratio (Spearman's rank test, $r=0.32$, $p<0.05$).

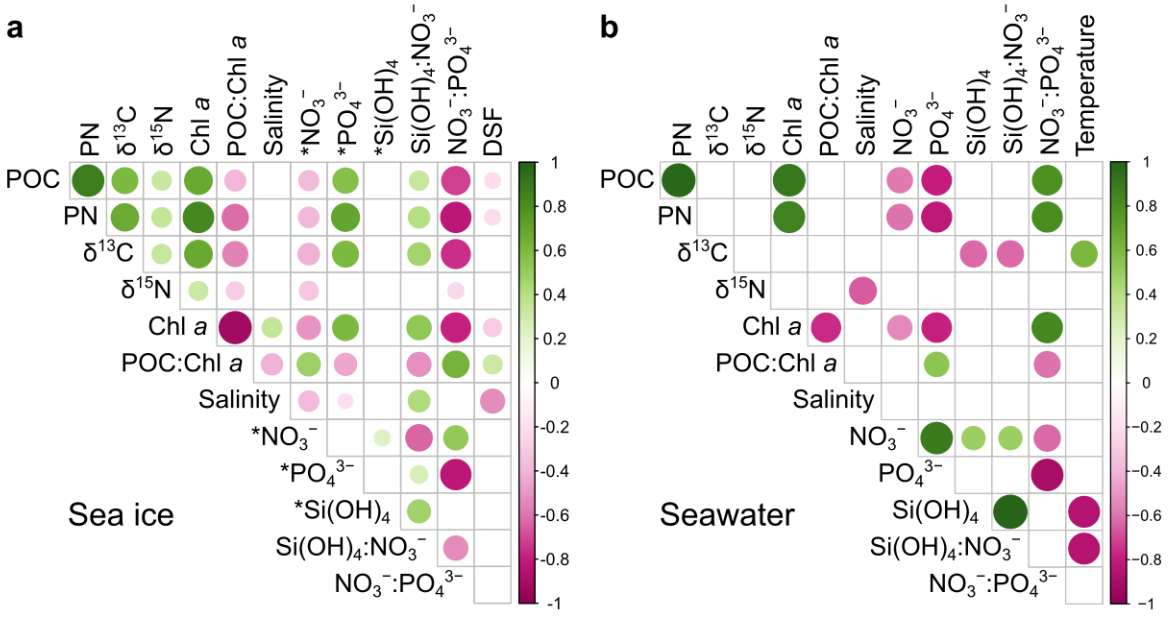

Figure 5: Inter-relationships of biogeochemical properties and POC, PN concentration and their isotopic ratios for sea ice and surface seawater. DSF: days since sea-ice formation.

The sea-ice POM $\delta^{13}C$ and $\delta^{15}N$ showed positive correlations with POC, PN, and Chl *a* concentration (Spearman's rank test, $r=0.30$, $p<0.05$), while they correlated negatively with POC:Chl *a* ($r=-0.57$ and $r=-0.28$ for $\delta^{13}C$ and $\delta^{15}N$, respectively, $p<0.05$). Among each nutrient, both $\delta^{13}C$ and $\delta^{15}N$ showed a negative correlation with $*NO_3^-$ and $NO_3^-:PO_4^{3-}$ (Spearman's rank test, $r<-0.20$, $p<0.05$), while only $\delta^{13}C$ showed a positive correlation with $*PO_4^{3-}$ and $Si(OH)_4:NO_3^-$.

The POC and PN concentrations in surface seawater also showed a strong positive correlation with the Chl *a* concentration (Spearman's rank test, $r=0.90$ and $r=0.87$ for POC and PN, respectively, $p<0.05$, Fig. 5b). However, unlike sea ice, they showed negative correlations with PO_4^{3-} (Spearman's rank test, $r<-0.78$, $p<0.05$). $\delta^{13}C$ showed a negative correlation with

https://doi.org/10.5194/egusphere-2026-2645
Preprint. Discussion started: 20 May 2026

$Si(OH)_4$ concentration and the $Si(OH)_4$:NO_3^- ratio (Spearman's rank test, $r<-0.63$, $p<0.05$), while $\delta^{13}C$ showed a positive one with sea surface temperature ($r=0.62$, $p<0.05$). $\delta^{15}N$ showed a significant negative correlation only with salinity (Spearman's rank test, $r=-0.66$, $p<0.05$).

3.5 Contribution of POC released from sea ice to the production in the water column

The POC_{VWM} concentration for sea ice (excluding newly formed ice) was 1137.6 μg L^{-1}, with an average value of 1353.0 μg L^{-1} and a median of 1022.1 μg L^{-1}. The POC supply from sea ice in the Indian sector, calculated from meltwater flux and the area of the SIZ, was 4.6±0.3 Tg $year^{-1}$ (Table 2). Assuming the primary production at the MIZ in this sector to be 27.9±5.0 Tg $year^{-1}$ (Arrigo et al., 2008), sea ice-derived carbon was found to account for 16.5±3.1% of this production. The Chl_{VWM} concentration was 12.0 μg L^{-1}. The POC_{algae} concentration estimated by POC_{VWM} and the mean IAC:Chl *a* ratio (54.4±26.5, Section 2.6) yielded 652.8±318.0 μg L^{-1}, which corresponds to 57.4±28.0% of POC_{VWM}.

Table 2: The estimated input of POC from sea ice and its contribution to primary production in the marginal ice zones of the Indian Sector of the Southern Ocean. The standard deviation (SD) for the contribution of sea-ice POC to the production in seawater was calculated by propagation of error using SD of POC input and primary production in the MIZ.

Variable	Estimates
POC_{VWM} (μg L^{-1})[a]	1137.6
Mean ice melt thickness in the Indian Sector (m)[b]	0.82
POC Input from ice per area (a×b, mg m^{-2} $year^{-1}$)	932.8
Seasonal sea-ice zone of the Indian sector (×10^6 km^2)[c]	4.9±0.3
POC Input from ice in the Indian Sector (Tg $year^{-1}$)[c]	4.6±0.3
Primary production in the MIZ and MIZ Shelf within the Indian Sector (Tg $year^{-1}$)[d]	27.9±5.0
Contribution of sea-ice POC to the primary production in MIZ (c÷d, %)	16.5±3.1

[a]Volume-Weightd Mean (VWM) of all sea-ice POC except newly formed ice, [e]Estimates from Komatsu et al. (2025), [c]Parkinson (2019), [d]Arrigo et al. (2008)

4 Discussion

4.1 Spatial and temporal variabilities of sea-ice particulate organic matter

Sea ice salinity, excluding newly formed ice, was negatively correlated with the days since sea-ice formation: DSF; this is likely due to desalination associated with surface melting and brine discharge during summer, as well as snow accumulation

https://doi.org/10.5194/egusphere-2026-2645
Preprint. Discussion started: 20 May 2026

(Eicken, 1992). Conversely, POC, PN, and Chl *a* concentrations gradually decreased as DSF increased (Fig. 6), although there is diversity among sea-ice samples. Our sea ice was collected during the summer season (December to February) when primary productivity is generally in a declining phase (net heterotrophy), as indicated by a decrease in total organic carbon (Dalman et al., 2025). Besides, high DSF (>200 days) may be responsible for the decline in POC, PN, and Chl *a* concentration given that Antarctic ice-algal biomass is deemed limited by light for ice with DSF <250 days (Raymond et al., 2009). In multi-year ice, nitrate concentration is much lower than first-year ice (Henley et al., 2023). In such environment, algal accumulation is slow, for the dissolution of diatom frustules ($Si(OH)_4$ accumulation) surpassed the consumption by diatoms (Sahashi et al., 2022). There was a weak but significant positive correlation between POC:Chl *a* and DSF, suggesting that in older (high DSF) samples, sea ice algae were at the senescent stage.

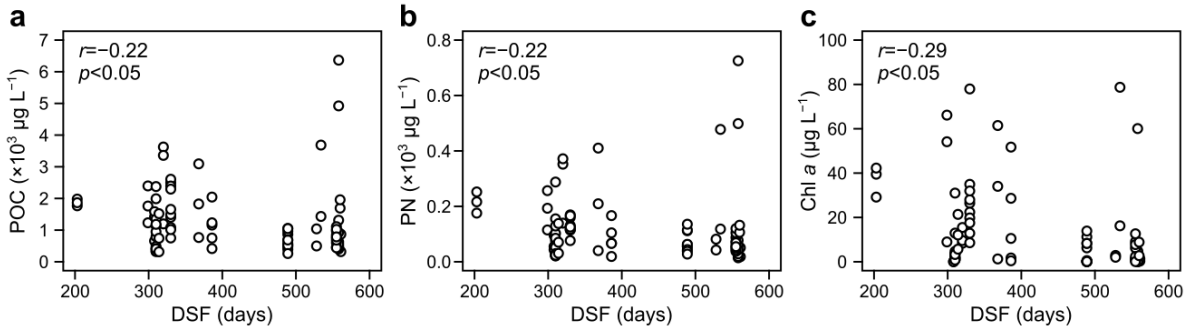

Figure 6: Relationships between days since sea-ice formation (DSF) at each station and the concentrations of POC (a), PN (b), Chl *a* (c) of sea ice. The Spearman's rank correlation coefficient and p-values are shown in the top left.

The maximum Chl *a* concentration in newly formed ice in the Southern Ocean is 260.0 µg L^{-1} (Ito et al., 2025), while the POC and Chl *a* concentrations in this study were 246.1–1354.0 µg L^{-1} and 0.2–4.0 µg L^{-1}, respectively (Fig. 3c, d). Therefore, the samples in this study were considered to have formed without active frazil ice production or phytoplankton blooms (Ito et al., 2025; Takahashi et al., 2025). Despite the low Chl *a* concentration, the newly formed ice exhibited high average POC:PN and POC:Chl *a* ratios, which were significantly higher than those of some FYI/OI samples, such as those in SC (Fig. 3e, h). This difference is likely due to differences in ice-algal composition and the selective accumulation of organic matter during sea-ice formation and growth. The newly formed ice sample from St. S138, which had the highest POC:Chl *a* ratio, was dominated by nanoflagellates (Takahashi et al., 2025). The POC:Chl *a* ratio for *Phaeocystis antarctica*, the predominant nanoflagellate in the Southern Ocean, ranges from 41 to 284 (Arrigo et al., 2010), and this is significantly higher than that for diatoms (approximately 37, Whitaker, 1977). In East Antarctic sea ice, diatoms dominate over nanoflagellates as the sea ice grows (Takahashi et al., 2025), suggesting that differences in algal composition contribute to the relatively high POC:Chl *a* ratio in newly formed ice than older ice. Another process that influences the POC:Chl *a* ratio is the selective incorporation of particulates during sea ice formation (Gradinger and Ikävalko, 1998; Janssens et al., 2016;

https://doi.org/10.5194/egusphere-2026-2645
Preprint. Discussion started: 20 May 2026

Takahashi et al., 2025). Since POC incorporation into sea ice is higher than PN and small (<10 µm) algal cells (Janssens et al., 2016), the dominance of small nanoflagellates in seawater (St. S138, Takahashi et al., 2025) could enhance POC:PN and POC:Chl *a* ratios in newly formed ice.

4.2 Driving factors of carbon and nitrogen isotope ratios in sea ice

The $\delta^{13}C$ of sea-ice POC was −24.3±3.1‰, higher than the $\delta^{13}C$ of surface seawater in the SIZ (−31‰ to −24‰, Espinasse et al., 2019, and −29±1.0‰ in this study). The $\delta^{15}N$ of sea-ice PN (1.5±2.1‰) was also generally higher than summer seawater (−5‰ to +7‰, Espinasse et al., 2019, −0.5±1.3‰ in this study). However, they remained within the range previously reported for Antarctic sea ice (Rau et al., 1991; Kennedy et al., 2002; Munro et al., 2010). The stable isotope ratios of particulate organic carbon in sea ice varied across the observed regions, likely due to differences in sea ice organic matter and nutrient concentrations among regions (Fig. 3). This section discusses drivers of stable isotope ratios in the context of sea-ice biogeochemical parameters.

Microalgae incorporate ^{13}C when CO_2 becomes limiting; hence, $\delta^{13}C$ of POM in sea-ice could increase under closed conditions and high algal CO_2 demand (i.e., when high ice-algal biomass is reached) (Kennedy et al., 2002). According to Nomura et al. (2023), the brine volume fraction in brash ice is 16.2%. Since this exceeds the threshold for gas permeability to the atmosphere (5%; Golden et al., 1998), $\delta^{13}C$ values could be distinct from those of more intact ice floes. However, our samples showed a significant positive correlation between sea-ice POC and $\delta^{13}C$, and high $\delta^{13}C$ values (>−20‰) were limited to high POC concentration (>2,000 µg L^{-1}), generally consistent with the previous sea-ice core observations (Kennedy et al., 2002; Munro et al., 2010) (Fig. 7). Three possible reasons for the similar isotope ratios between brash ice and ice floes are as follows: 1) brash ice reflects the history of the ice floes before they are broken, 2) there is limited exchange between sea ice and the atmosphere at the microscale, and 3) dilution of brine DIC by surface melting of brash ice. For reason 1, although there are no direct measurements of productivity in brash ice, reports indicate net heterotrophic activity in late-summer (February) sea ice (Dalman et al., 2025). Thus, the isotope ratios during earlier periods (i.e., when sea ice was not broken into brash ice) may have been recorded in our brash sea ice samples. According to the field observation in spring Antarctic sea ice, $\delta^{13}C$ increases with algal accumulation in the very surface layer of sea ice (5 cm inside sea ice from ice–water interface, McMinn et al., 1999), which could be the reason 2). For this reason, 3, pCO_2 in sea ice declines with increasing brine volume fraction (Nomura et al., 2010; Geilfus et al., 2014; van der Linden et al., 2020). As pack ice breaks up into smaller pieces, it warms by approaching the temperature of seawater. As brine salinity decreases and DIC dilution in the brine progresses, CO_2 can become rate-limiting in brash ice (Nomura et al., 2010). However, the brine salinity of broken ice derived from ice temperature is 27.6±4.8 (Nomura et al., 2023; Vancoppenolle et al., 2019), indicating the dilution effect is not significant to determine brash ice $\delta^{13}C$.

https://doi.org/10.5194/egusphere-2026-2645
Preprint. Discussion started: 20 May 2026

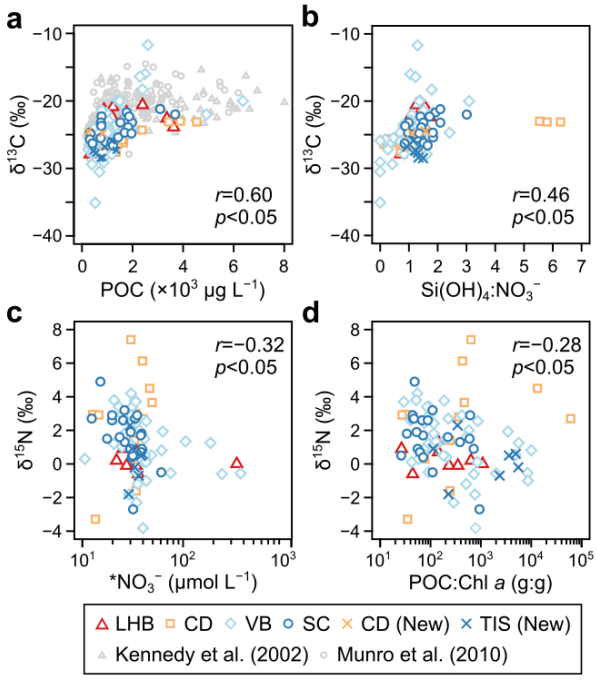

Figure 7: Relationships of $\delta^{13}C$ and POC concentration (a), $\delta^{13}C$ and $Si(OH)_4:NO_3^-$ (b), $\delta^{15}N$ and $*NO_3^-$ concentration (c), and $\delta^{15}N$ and POC:Chl *a* (d). The grey triangles and circles are derived from sea-ice data of Kennedy et al. (2002) and Munro et al. (2010), respectively. The Spearman's rank correlation coefficient and p-values are shown in the bottom or top right.

Within sea ice, PO_4^{3-} is regenerated alongside diatom proliferation, resulting in extremely low summer $NO_3^-:PO_4^{3-}$ ratios (Fripiat et al., 2017; Takahashi et al., 2022; Nomura et al., 2023). Due to PO_4^{3-} regeneration, a negative correlation exists between ice-algal biomass, in particular diatoms, and $NO_3^-:PO_4^{3-}$ ratios in brash ice (Takahashi et al., 2022). In this study, a negative correlation between $\delta^{13}C$ and $NO_3^-:PO_4^{3-}$ was observed, suggesting that diatoms contributed to the $\delta^{13}C$ increase. Furthermore, previous microscopic observations of East Antarctic sea ice have confirmed that diatoms dominate during late spring and summer (Meiners et al., 2011; Takahashi et al., 2022; 2023; 2025). On the other hand, the negative correlation between $\delta^{13}C$ and $Si(OH)_4:NO_3^-$ suggests that different diatom species in sea ice may exhibit distinct ^{13}C isotope fractionation (Burkhardt et al., 1999). Fischer et al. (1991) investigated the surface POC $\delta^{13}C$ distribution in the Scotia Sea and reported a positive correlation between the particulate Si:N ratio and $\delta^{13}C$. Diatoms have different silica requirements depending on the species. For example, the $Si(OH)_4$ half-saturation constant of *Corethron pennatum* is more than ten times that of small diatoms (Sommer and Stabel, 1986). Large diatoms with high particulate Si:N ratios (i.e., those that induce low $Si(OH)_4:NO_3^-$) incorporate relatively little ^{13}C (Burkhardt et al., 1999; Fischer et al., 1991), suggesting that differences in diatom taxa within sea ice may be reflected in the variation of $\delta^{13}C$ values. However, the correlation coefficient between $\delta^{13}C$

https://doi.org/10.5194/egusphere-2026-2645
Preprint. Discussion started: 20 May 2026

and $Si(OH)_4$:NO_3^- (r=−0.53) is lower than those with POC, PN, or Chl *a* concentrations, suggesting a smaller effect on the increase in $\delta^{13}C$ than algal accumulation.

According to studies on the stable isotope ratios of POM in seawater, nitrogen nutrient utilization reflects variations in PN $\delta^{15}N$ (Saino and Hattori, 1980). Nomura et al. (2023) reported that despite brash ice having high permeability and exchange with seawater (>5% brine volume fraction), the biological activity in sea ice influences the nutrient concentration. In this study, PO_4^{3-} was highly enriched in sea ice, while $Si(OH)_4$, known for its slow decomposition rate, was lower than in seawater (Fig. 2e, f). Due to these characteristics, even brash ice subject to melting has a distinct nutrient status within the ice compared to seawater, which likely contributed to the observed $\delta^{15}N$ values. In this study, $\delta^{15}N$ showed a negative correlation with $*NO_3^-$, suggesting that nitrogen consumption contributed to the high isotope ratio. Diatoms selectively incorporate ^{14}N (Wada and Hattori, 1978), hence, in a closed system where NO_3^- is actively consumed, the $\delta^{15}N$ of remaining (unconsumed) NO_3^- increases (Wu et al., 1997). The uptake of NO_3^- is supported by the negative correlations between POC, PN, and Chl *a* concentrations and $*NO_3^-$ (Fig. 5).

Conversely, it is known that $\delta^{15}N$ values of PN or dissolved inorganic nitrogen also change during organic matter decomposition and nitrification (oxidation from NH_4^+ to oxidized nitrogen species) (Saino and Hattori, 1980). The POC:Chl *a* ratio in this study showed a negative correlation with $\delta^{15}N$. An increase in the POC:Chl *a* ratio is linked to NH_4^+ accumulation from predation and excretion by heterotrophic organisms (Schnack-Schiel et al., 2004) and remineralization of particulate organic matter (Roukaerts et al., 2021). Although $\delta^{15}N$ decreases during the oxidation of NH_4^+ to NO_2^- through the fractionation by nitrifying bacteria, ^{15}N accumulates in NO_3^- during the subsequent oxidation of NO_2^- to NO_3^- (Casciotti et al., 2003; 2009). Therefore, NO_3^- produced by nitrification is considered to have $\delta^{15}N$ values similar to or lower than those of NH_4^+ produced by decomposition (i.e., NH_4^+ before its nitrification) (Henley et al., 2018). On the other hand, when algae directly assimilate NH_4^+, the $\delta^{15}N$ of PN decreases due to the lower fractionation factor, −25‰ and −15‰ (negative values indicate greater incorporation of ^{14}N into the algae) than nitrification (Waser et al., 1998). The nitrification rate in sea ice is known to correlate positively with Chl *a* concentration (Priscu et al., 1990). In this study, POC:Chl *a* was negatively correlated with Chl *a* concentration (Fig. 5a). That is, higher POC:Chl *a* ratios in sea ice may have been associated with reduced nitrification activity. The negative correlation between POC:Chl *a* ratio and $\delta^{15}N$ (Fig. 7d) suggests that even if NH_4^+ may be re-mineralized due to the shift from autotrophy to heterotrophy, direct NH_4^+ utilization by ice algae likely outweighed assimilation after nitrification of NH_4^+ (conversion of NH_4^+ to NO_3^-) and resulted in low PN $\delta^{15}N$. This hypothesis is supported by observations showing relatively high NH_4^+ uptake rates in the upper layer of Antarctic drift ice, where the POC:Chl *a* ratio is higher than that in the interior or bottom sections of sea ice (Roukaerts et al., 2016).

4.3 Contribution of ice algae on particulate organic carbon in sea ice

https://doi.org/10.5194/egusphere-2026-2645
Preprint. Discussion started: 20 May 2026

The POC:Chl *a* ratio varied significantly across regions, seasons, and sea-ice types (FY/OI and newly formed ice). This result indicates that carbon sources other than ice algae are also important for the POC consumed by pelagic heterotrophs in the water column during sea ice melt. The relationship between POC and Chl *a* concentrations (Fig.2c) showed that sea ice with high C_{algae} contributions (sample plots above the IAC:Chl *a*=54.4 line) was most common in sea ice with low to moderate Chl *a* concentrations (<30 μg L^{-1}); this aligns with previous reports that ice algae contribute most of the carbon in sea ice with extremely high Chl *a* concentrations (Takahashi et al., 2023). The POC:Chl *a* ratio showed a tendency to increase from December to February, and the POC:Chl *a* ratio was found to have a significant positive correlation with days since formation (DSF). These findings indicate that from early to late summer, older sea ice contributes to a greater proportion of non-algal-derived POC.

Although the types of non-algal-derived POC were not identified, one possibility is the presence of extracellular polymeric substances (EPS) or detritus within ice (Dumont et al., 2009). Studies examining temporal changes in sea-ice EPS and Chl *a* concentrations have reported that EPS tends to remain within the ice longer than Chl *a* during the melting season (Riedel et al., 2008). In general, EPS forms biofilms that cause ice algae and bacteria to attach within brine pockets, preventing particulate matter from following brine dynamics (i.e., salinity decreases during melting). In this study, although a weak positive correlation existed between Chl *a* concentration and salinity, POC and PN showed no relationship with salinity. Therefore, in older sea ice, some portions of ice algae (Chl *a*) may have been released through brine expulsion, whereas POC likely remained on the ice. The negative correlation between the POC:Chl *a* ratio and Chl *a* concentration supports the notion that Chl *a* is more readily decomposed or removed from sea ice than POC or PN.

4.4 Potential impact of ice particulate organic matter during the melting season

Based on the measured sea ice POC concentrations and sea ice melt fluxes, the impact of sea ice-derived carbon on marine zooplankton as a food resource during the melt season was estimated (Table 2). When combined with primary production after ice retreat, POC from sea ice accounted for 16.5±3.1% of primary production in the MIZ of the studied sector. It should be noted that since POC concentrations in sea ice during October–November—before the observation period of this study—were not included, calculations solely using summer sea-ice data may have resulted in an overestimation of the POC supply. Nevertheless, according to satellite-based estimates by Bocquet et al. (2024), approximately 85% of sea-ice melt (sea-ice volume reduction) occurs between December and February. Therefore, even if we excluded the POC supply from October to November, the summer POC from melted sea ice is equivalent to 14.1% of production in the MIZ.

The previous estimate of POC supply from sea ice was 0.252 Tg C $year^{-1}$ in the Weddell Sea (60°W–30°E), calculated from sea ice extent and POC concentrations converted from sea-ice Chl *a* (Ackley et al., 1979). When estimated per unit area, this corresponds to 35.7 mg m^{-2} $year^{-1}$, which is significantly lower than our estimate of 924 mg m^{-2} $year^{-1}$ (Table 2). This difference may be attributed to the conservative assumptions used by Ackley et al. (1979), who averaged the low sea-ice Chl

https://doi.org/10.5194/egusphere-2026-2645
Preprint. Discussion started: 20 May 2026

a concentration (1.2 mg m^{-2}) over February and March. However, recent reports found an average sea-ice Chl *a* concentration of 6.4 mg m^{-2} across the Antarctic SIZ, which increases to 12.8 mg m^{-2} during February to March (Meiners et al., 2012). It should also be noted that the POC:Chl *a* ratio was 37 in the previous estimate, which is close to the lower limit observed during ice algal blooms (Whitaker, 1977). The POC:Chl *a* ratio can exceed 100 in spring sea ice (Roukaerts et al., 2016), and the median FYI/OI in this study was 170, possibly because of EPS and detritus. Given the differences between these assumptions, the POC supply from sea ice is one to two orders of magnitude higher than that estimated by Ackley et al. (1979), which is closer to our estimate.

Finally, we discuss the impact of POC supply from sea ice on the carbon content in the water column from the perspective of primary consumers. Antarctic filter-feeding euphausiids (*Euphausia superba*, *E. crystallorophias*, *Thysanoessa macrura*) have been reported to consume ice algae which constitute 5–36% (11% on average) of the carbon in their diet in the summer MIZ (Kohlbach et al., 2019). The contribution of sea-ice POM to zooplankton diets may depend on the vertical distribution of zooplankton (Kohlbach et al., 2019) and the spatiotemporally heterogeneous occurrence of ice-edge blooms (Fitch and Moore, 2007). Our estimate (>14% of MIZ production), which was temporally integrated, fell within this range. In this study, the POC:PN ratio was >10 on average, indicating lower food quality than phytoplankton (surface seawater POM, 5.2±0.5 POC:PN ratio in this study). Daase et al. (2011) found that copepods fed phytoplankton with high POC:PN ratios failed to reach the copepodite stage at low temperatures (−1.2°C). However, the growth time and body size during the nauplius stage were equivalent to those when fed high-quality (low POC:PN ratio) food (Daase et al., 2011). Therefore, POM from sea ice during the summer is thought to support the growth of zooplankton larvae (such as copepod nauplii).

5 Conclusions

This study is the first to reveal the isotopic signatures of POM in brash sea ice and its distribution across an extensive SIZ in the Southern Ocean. When averaged for all POM data, no significant differences in sea-ice $\delta^{13}C$ and $\delta^{15}N$ were observed during summer. This finding suggests that the isotope ratios obtained in this study can aid estimating the food webs in the summer MIZ from previously accumulated zooplankton isotope ratio datasets (e.g., Liu and Zhou, 2025). While particulate accumulation (POM and Chl *a* concentrations) primarily contributed to variations in isotope ratios, nutrient uptake by ice algae also influenced them. This implies that changes in ice-algal species composition associated with variations in East Antarctic sea ice (e.g., ice thickness and snow accumulation) may alter sea-ice isotope ratios. The POC:Chl *a* ratio and POC concentration in sea ice showed correlations with the DSF, indicating that the quantity or quality of POM and the subsequent supply from ice also may change with sea ice age and drift. Furthermore, we estimated the carbon supply from sea ice to be 4.6±0.3 Tg C $year^{-1}$, equivalent to 16.5±3.1% of primary production in the MIZ. Because this carbon includes contributions from sources other than ice algae themselves (43% on average), it is necessary to investigate the composition of these carbon sources (lipids, EPS, etc.) and their contributions within the food web in detail.

https://doi.org/10.5194/egusphere-2026-2645
Preprint. Discussion started: 20 May 2026

Data availability

The physico-chemical and biological data of sea ice (https://ads.nipr.ac.jp/dataset/A20260507-001) and sea-ice motion data (http://doi.org/10.17592/001.2025112601) are archived in the Arctic and Antarctic Data Archive System (ADS) managed by National Institute of Polar Research, Japan. A DOI for the sampled sea ice will be included in the final version of the manuscript upon publication.

Author contributions

Conceptualization: RM, KDT; Investigation: KDT, RM, MS, KN, NK, DN, MYK, RM, NN, MI, ST, NMH, AT, NK, TT, KIO, KM, SA, MM; Formal analysis: KDT, RM, MS, KN, NK, DN, MYK, RM, NN, MI, ST, NMH, AT, NK, MK; Funding acquisition: KDT, RM, MI, NK, TT, MK, KIO, SA, MM; Writing – original draft: KDT, RM; Writing – review & editing: All authors

Competing interests

The authors declare that they have no competing interests regarding in this study.

Disclaimer

Copernicus Publications remains neutral with regard to jurisdictional claims made in the text, published maps, institutional affiliations, or any other geographical representation in this paper. While Copernicus Publications makes every effort to include appropriate place names, the final responsibility lies with the authors. Views expressed in the text are those of the authors and do not necessarily reflect the views of the publisher.

Acknowledgements

We thank the captain and crew of the T/V *Umitaka-maru*, R/V *Hakuho-maru*, and ice breaker *Shirase* for their support during the cruises. Our appreciation goes to Dr. Tsuneo Odate for his supports on the Antarctic research expeditions. The data points from Fig. 7c were obtained and modified from Munro et al. (2010) with a permission by AGU Publications, John Wiley and Sons. An open AI tool was used to assist the translation and preparation for the first manuscript.

https://doi.org/10.5194/egusphere-2026-2645
Preprint. Discussion started: 20 May 2026

Financial support

This study was supported by JSPS KAKENHI Grant Nos. 24KJ0006, 21J14914, and 24K17997 to K.D. Takahashi, 20H04313, 22H05003, and 24H00759 to R. Makabe, 17H06319 to M. Moteki, 17H06317 and 20H05707 to K.I. Ohshima, 16101001 to T. Odate, and JST CREST Grant Number JPMJCR23J5, Japan. The field observations were supported by the funds of the National Institute of Polar Research (Project Research, No. KP-308 to T. Odate), and Japanese Antarctic Research Expedition (Ordinary Research Projects, No. AP-0923, and No. AP-0939 to M. Moteki and Prioritized Research Projects, AJ-0902 to S. Aoki, and AJ-1003 to K. Mizobata). This research was supported by the Cooperative Programs, JURCAOSKAV19-57, JURCAOSKAV20-56, JURCAOSKAV22-50, JURCAOSKAV23-48 of Atmosphere and Ocean Research Institute, The University of Tokyo. This study was supported partly by the Grant for Joint Research Program of the Institute of Low Temperature Science, Hokkaido University (22S012, 23S017, 24S015, and 25S010).

References

Ackley, S. F., Buck, K. R., and Taguchi, S.: Standing crop of algae in the sea ice of the Weddell Sea region, Deep-Sea Res. A. Oceanogr. Res. Pap., 26(3), 269–281, https://doi.org/10.1016/0198-0149(79)90024-4, 1979.

Akino, R., Nomura, D., Sahashi, R., Tozawa, M., Hatta, M., Matsuno, K., Endo, W., Shiozaki, T., Kawakami, T., Ito, M., Murata, A., and Fujiwara, A.: Characteristics of late summer Arctic brash sea ice and its melting effect on the surface-water biogeochemistry of the Chukchi Shelf and Canada Basin. Elem. Sci. Anth., 12, 00094, https://doi.org/10.1525/elementa.2023.00094, 2024.

Ardyna, M., Claustre, H., Sallée, J. B., D'Ovidio, F., Gentili, B., van Dijken, G., D'Ortenzio, F., and Arrigo, K. R.: Delineating environmental control of phytoplankton biomass and phenology in the Southern Ocean, Geophys. Res. Lett., 44, 5016–5024, https://doi.org/10.1002/2016GL072428, 2017.

Arrigo, K. R., van Dijken, G. L., and Bushinsky, S.: Primary production in the Southern Ocean, 1997–2006, J. Geophys. Res., 113(C8), C08004, https://doi.org/10.1029/2007jc004551, 2008.

Arrigo, K. R., Mills, M. M., Kropuenske, L. R., Van Dijken, G. L., Alderkamp, A.-C., and Robinson, D. H.: Photophysiology in two major Southern Ocean phytoplankton taxa: Photosynthesis and growth of *Phaeocystis antarctica* and *Fragilariopsis cylindrus* under different irradiance levels, Integr. Comp. Biol., 50(6), 950–966, https://doi.org/10.1093/icb/icq021, 2010.

https://doi.org/10.5194/egusphere-2026-2645
Preprint. Discussion started: 20 May 2026

Becquevort, S., Dumont, I., Tison, J. L., Lannuzel, D., Sauvée, M. L., Chou, L., and Schoemann, V.: Biogeochemistry and microbial community composition in sea ice and underlying seawater off East Antarctica during early spring, Polar Biol., 32(6), 879–895, https://doi.org/10.1007/s00300-009-0589-2, 2009.

Bocquet, M., Fleury, S., Rémy, F., and Piras, F.: Arctic and Antarctic sea ice thickness and volume changes from observations between 1994 and 2023, J. Geophys. Res.: Oceans, 129(11), e2023JC020848, https://doi.org/10.1029/2023JC020848, 2024.

Burkhardt, S., Riebesell, U., and Zondervan, I.: Stable carbon isotope fractionation by marine phytoplankton in response to daylength, growth rate, and CO_2 availability, Mar. Ecol. Prog. Ser., 184, 31–41, https://doi.org/10.3354/meps184031, 1999.

Casciotti, K. L., Sigman, D. M., and Ward, B. B.: Linking diversity and stable isotope fractionation in ammonia-oxidizing bacteria, Geomicrobiol. J., 20(4), 335–353, https://doi.org/10.1080/01490450303895, 2003.

Casciotti, K. L.: Inverse kinetic isotope fractionation during bacterial nitrite oxidation, Geochim. Cosmochim. Acta., 73(7), 2061–2076, https://doi.org/10.1016/j.gca.2008.12.022, 2009.

Corkill, M., Moreau, S., Janssens, J., Fraser, A. D., Heil, P., Tison, J. L., Cougnon, E. A., Genovese, C., Kimura, N., Meiners, K. M., Wongpan, P., and Lannuzel, D.: Physical and biogeochemical properties of rotten East Antarctic summer sea ice, J. Geophys. Res.: Oceans, 128(2), e2022JC018875, https://doi.org/10.1029/2022JC018875, 2023.

Daase, M., Søreide, J. E., and Martynova, D. Effects of food quality on naupliar development in Calanus glacialis at subzero temperatures, Mar. Ecol. Prog. Ser., 429, 111-124, 2011.

Dalman, L. A., Meiners, K. M., Thomas, D. N., Deman, F., Bestley, S., Moreau, S., Arrigo, K. R., Campbell, K., Corkill, M., Cozzi, S., Delille, B., Munro, D. R., Nomura, D., Norman, L., Papadimitriou, S., Schallenberg, C., Tison, J.-L., Vancoppenolle, M., van der Merwe, P., and Fripiat, F.: Observation-based estimate of net community production in Antarctic sea ice, Geophys. Res. Lett., 52, e2024GL113717, https://doi.org/10.1029/2024GL113717, 2025.

Dieckmann, G. S., Eicken, H., Haas, C., Garrison, D. L., Gleitz, M., Lange, M., Spindler, M., Sullivan, C. W., Thomas, D. N., Weissenberger, J. N.: A compilation of data on sea ice algal standing crop from the Bellinghausen, Amundsen and Weddell Seas from 1983 to 1994, in: Antarctic sea ice: Biological Processes, Interactions and Variability, edited by: Lizotte, M. P., and Arrigo, K. R., American Geophysical Union, Washington, US, 85–92, https://doi.org/10.1029/AR073p0085, 1998.

https://doi.org/10.5194/egusphere-2026-2645
Preprint. Discussion started: 20 May 2026

Dumont, I., Schoemann, V., Lannuzel, D., Chou, L., Tison, J.-L., and Becquevort, S.: Distribution and characterization of dissolved and particulate organic matter in Antarctic pack ice, Polar Biol., 32(5), 733–750, https://doi.org/10.1007/s00300-008-0577-y, 2009.

Eayrs, C., Li, X., Raphael, M. N., and Holland, D. M.: Rapid decline in Antarctic sea ice in recent years hints at future change, Nat. Geosci., 14(7), 460–464, https://doi.org/10.1038/s41561-021-00768-3, 2021.

Eicken, H.: Salinity profiles of Antarctic sea ice: Field data and model results, J. Geophys. Res., 97(C10), 15545–15557, https://doi.org/10.1029/92JC01588, 1992.

Espinasse, B., Pakhomov, E. A., Hunt, B. P. V., and Bury, S. J.: Latitudinal gradient consistency in carbon and nitrogen stable isotopes of particulate organic matter in the Southern Ocean, Mar. Ecol. Prog. Ser., 631, 19–30. https://doi.org/10.3354/meps13137, 2019.

Fitch, D. T., and Moore J. K.: Wind speed influence on phytoplankton bloom dynamics in the Southern Ocean marginal ice zone, J. Geophys. Res.: Oceans, 1112, C08006, https://doi.org/10.1029/2006JC004061, 2007.

Fischer, G.: Stable carbon isotope ratios of plankton carbon and sinking organic matter from the Atlantic sector of the Southern Ocean, Mar. Chem., 35(1–4), 581–596, https://doi.org/10.1016/S0304-4203(09)90044-5, 1991.

Frölicher, T. L., Sarmiento, J. L., Paynter, D. J., Dunne, J. P., Krasting, J. P., and Winton, M.: Dominance of the Southern Ocean in anthropogenic carbon and heat uptake in CMIP5 models, J. Clim., 28(2), 862–886, https://doi.org/10.1175/jcli-d-14-00117, 2015.

Fripiat, F., Meiners, K. M., Vancoppenolle, M., Papadimitriou, S., Thomas, D. N., Ackley, S. F., Arrigo, K. R., Carnat, G., Cozzi, S., Delille, B., Dieckmann, G. S., Dunbar, R. B., Fransson, A., Kattner, G., Kennedy, H., Lannuzel, D., Munro, D. R., Nomura, D., Rintala, J.-M., Schoemann, V., Stefels, J., Steiner, N., Tison, J.-L.: Macro-nutrient concentrations in Antarctic pack ice: Overall patterns and overlooked processes, Elem. Sci. Anthropocene, 5, 13, https://doi.org/10.1525/elementa.217, 2017.

Geilfus, N.-X., Tison, J.-L., Ackley, S. F., Galley, R. J., Rysgaard, S., Miller, L. A., and Delille, B.: Sea ice pCO_2 dynamics and air—Ice CO_2 fluxes during the sea ice mass balance in the Antarctic (SIMBA) experiment—Bellingshausen Sea, Antarctica, Cryosphere, 8(6), 2395–2407, https://doi.org/10.5194/tc-8-2395-2014, 2014.

https://doi.org/10.5194/egusphere-2026-2645
Preprint. Discussion started: 20 May 2026

Golden, K. M., Ackley, S. F., and Lytle, V. I.: The Percolation Phase Transition in Sea Ice, Science, 282, 2238–2241, https://doi.org/10.1126/science.282.5397.2238, 1998.

Gradinger, R., and Ikävalko, J.: Organism incorporation into newly forming Arctic sea ice in the Greenland Sea, J. Plankton Res., 20(5), 871–886, https://doi.org/10.1093/plankt/20.5.871, 1998.

Henley, S. F., Jones, E. M., Venables, H. J., Meredith, M. P., Firing, Y. L., Dittrich, R., Heiser, S., Stefels, J., and Dougans, J. Macronutrient and carbon supply, uptake and cycling across the Antarctic Peninsula shelf during summer, Philos. Trans. A Math. Phys. Eng. Sci., 376(2122), 20170168. https://doi.org/10.1098/rsta.2017.0168, 2018.

Henley, S. F., Cozzi, S., Fripiat, F., Lannuzel, D., Nomura, D., Thomas, D. N., Meiners, K. M., Vancoppenolle, M., Arrigo, K., Stefels, J., van Leeuwe, M., Moreau, S., Jones, E. M., Fransson, A., Chierici, M., and Delille, B.: Macronutrient biogeochemistry in Antarctic land-fast sea ice: Insights from a circumpolar data compilation, Mar. Chem., 257, 104324, https://doi.org/10.1016/j.marchem.2023.104324, 2023.

Hersbach, H., Bell, B., Berrisford, P., Biavati, G., Horányi, A., Muñoz Sabater, J., Nicolas, J., Peubey, C., Radu, R., Rozum, I., Schepers, D., Simmons, A., Soci, C., Dee, D., Thépaut, J.-N.: ERA5 hourly data on single levels from 1959 to present [Dataset], Copernicus Climate Change Service (C3S) Climate Data Store (CDS). https://doi.org/10.24381/cds.adbb2d47, 2018.

Hersbach, H., Bell, B., Berrisford, P., Hirahara, S., Horányi, A., Muñoz-Sabater, J., Nicolas, J., Peubey, C., Radu, R., Schepers, D., Simmons, A., Soci, C., Abdalla, S., Abellan, X., Balsamo, G., Bechtold, P., Biavati, G., Bidlot, J., Bonavita, M., De Chiara, G., Dahlgren, P., Dee, D., Diamantakis, M., Dragani, R., Flemming, J., Forbes, R., Fuentes, M., Geer, A., Haimberger, L., Healy, S., Hogan, R. J., Hólm, E., Janisková, M., Keeley, S., Laloyaux, P., Lopez, P., Lupu, C., Radnoti, G., de Rosnay, P., Rozum, I., Vamborg, F., Villaume, S., and Thépaut, J.-N.: The ERA5 global reanalysis, Q. J. Roy. Meteor. Soc., 146, 1999–2049, https://doi.org/10.1002/qj.3803, 2020.

Ito, M., Takahashi, K. D., Makabe, R., Hirano, D., Ohshima, K. I., Tamura, T., and Aoki, S.: Intense frazil ice production promotes high algal biomass in newly-formed sea ice. J. Geophys. Res.: Oceans, 130(3), e2024JC021689, https://doi.org/10.1029/2024JC021689, 2025.

https://doi.org/10.5194/egusphere-2026-2645
Preprint. Discussion started: 20 May 2026

Janssens, J., Meiners, K. M., Tison, J.-L., Dieckmann, G., Delille, B., Lannuzel, D., and Miller, L. A.: Incorporation of iron and organic matter into young Antarctic sea ice during its initial growth stages, Elem. Sci. Anthropocene, 4, 000123, https://doi.org/10.12952/journal.elementa.000123, 2016.

Jia, Z., Swadling, K., Meiners, K., Kawaguchi, S., and Virtue, P.: The zooplankton food web under East Antarctic pack ice – A stable isotope study, Deep-Sea Res. Part II Top. Stud. Oceanogr., 13, 189–202, https://doi.org/10.1016/j.dsr2.2015.10.010, 2016.

Kennedy, H., Thomas, D. N., Kattner, G., Haas, C., & Dieckmann G. S.: Particulate organic matter in Antarctic summer sea ice: Concentration and stable isotopic composition, Mar. Ecol. Prog. Ser., 238, 1–13, https://doi.org//10.3354/meps238001, 2002.

Kimura, N.: Sea ice motion in response to surface wind and ocean current in the Southern Ocean, J. Meteor. Soc. Jpn. Ser. II, 82(4), 1223–1231, https://doi.org/10.2151/jmsj.2004.1223, 2004.

Kohlbach, D., Graeve, M., Lange, B. A., David, C., Schaafsma, F. L., van Franeker, J. A., Vortkamp, M., Brandt, A., and Flores, H.: Dependency of Antarctic zooplankton species on ice algae-produced carbon suggests a sea ice-driven pelagic ecosystem during winter, Glob. Change Biol., 24, 4667–4681, https://doi.org/10.1111/gcb.14392, 2018.

Kohlbach, D., Lange, B. A., Graeve, M., Vortkamp, M., and Flores. H.: Varying dependency of Antarctic euphausiids on ice algae- and phytoplankton-derived carbon during summer, Mar. Biol., 166, https://doi.org/10.1007/s00227-019-3527-z, 2019.

Komatsu, M., Ohshima, K. I., Mensah, V., and Nakata, K.: Mapping of sea-ice melting and net freshwater flux by sea-ice in the Southern Ocean, Commun. Earth Environ., 6(1), 579, https://doi.org/10.1038/s43247-025-02560-2, 2025.

Liu, Z., and Zhou, M.: Spatial variability of ice krill, *Euphausia crystallorophias*, diet from the Amundsen Sea to Ross Sea (Antarctica) revealed by stomach content and stable isotope analyses, Polar Biol., 48(4), 116, https://doi.org/10.1007/s00300-025-03438-x, 2025.

Makabe, R., Tanimura, A., Tamura, T., Hirano, D., Shimada, K., Hashihama, F., and Fukuchi, M.: Meso-zooplankton abundance and spatial distribution off Lützow-Holm Bay during austral summer 2007–2008, Polar Sci., 12, 25–33, https://doi.org/10.1016/j.polar.2016.09.002, 2017.

https://doi.org/10.5194/egusphere-2026-2645
Preprint. Discussion started: 20 May 2026

McMinn, A., Skerratt, J., Trull, T., Ashworth, C., and Lizotte, M.: Nutrient stress gradient in the bottom 5 cm of fast ice, McMurdo Sound, Antarctica, Polar Biol., 21, 220–227, https://doi.org/10.1007/s003000050356, 1999.

Meiners, K. M., Norman, L., Granskog, M. A., Krell, A., Heil, P., and Thomas, D. N.: Physico-ecobiogeochemistry of East Antarctic pack ice during the winter-spring transition, Deep-Sea Res. Part II Top. Stud. Oceanogr., 58(9–10), 1172–1181, https://doi.org/10.1016/j.dsr2.2010.10.033, 2011.

Meiners, K. M., Vancoppenolle, M., Shanassekos, S., Dieckmann, D. S., Thomas, D. N., Tison, J.-L., Arrigo, K. R., Garrison, D., McMinn, A., Lannuzel, D., van der Merwe, P., Swadling, K. M., Smith Jr., W. O., Melnikov, I., and Raymond, B.: Chlorophyll *a* in Antarctic sea ice from historical ice core data, Geophys. Res. Lett., 39, 21602–21602, https://doi.org/10.1029/2012GL053478, 2012.

Mincks, S. L., Smith, C. R., Jeffreys, R. M., and Sumida, P. Y. G.: Trophic structure on the West Antarctic Peninsula shelf: Detritivory and benthic inertia revealed by $\delta^{13}C$ and $\delta^{15}N$ analysis, Deep-Sea Res. Part II Top. Stud. Oceanogr., 55(22), 2502–2514, https://doi.org/10.1016/j.dsr2.2008.06.009, 2008.

Moreau, S., Boyd, P. W., and Struttom, P. G.: Remote assessment of the fate of phytoplankton in the Southern Ocean sea-ice zone, Nat. Commun., 11, 3108, https://doi.org/10.1038/s41467-020-16931-0, 2020.

Munro, D. R., Dunbar, R. B., Mucciarone, D. A., Arrigo, K. R., and Long, M. C.: Stable isotope composition of dissolved inorganic carbon and particulate organic carbon in sea ice from the Ross Sea, Antarctica, J. Geophys. Res.: Oceans, 115, C09005, https://doi.org/10.1029/2009JC005661, 2010.

Nakata, K., Ohshima, K. I., and Nihashi, S.: Estimation of thin ice thickness and discrimination of ice type from AMSR-E passive microwave data, IEEE Trans. Geosci. Remote Sens., 57(1), 263–276, https://doi.org/10.1109/TGRS.2018.2853590, 2019.

Nakata, K., Ohshima, K. I., and Nihashi, S.: Mapping of active frazil for Antarctic coastal polynyas, with an estimation of sea-ice production, Geophys. Res. Lett., 48(6), e2020GL091353, https://doi.org/10.1029/2020GL091353, 2021.

Nomura, D., Yoshikawa-Inoue, H., Toyota, T., and Shirasawa, K.: Effects of snow, snowmelting and refreezing processes on air–sea-ice CO_2 flux, J. Glaciol., 56, 262–270, https://doi.org/10.3189/002214310791968548, 2010.

https://doi.org/10.5194/egusphere-2026-2645
Preprint. Discussion started: 20 May 2026

Nomura, D., Granskog, M. A., Assmy, P., Simizu, D., and Hashida, G.: Arctic and Antarctic sea ice acts as a sink for atmospheric CO_2 during periods of snowmelt and surface flooding, J. Geophys. Res.: Oceans, 118, 6511–6524, https://doi.org/10.1002/2013JC009048, 2013.

Nomura, D., Sahashi, R., Takahashi, K.D., Makabe, R., Ito, M., Tozawa, M., Wongpan, P., Matsuda, R., Sano, M., Yamamoto-Kawai, M., Nojiro, N., Tachibana, A., Kurosawa, N., Moteki, M., Tamura, T., Aoki, S., and Murase, H.: Biogeochemical characteristics of brash sea ice and icebergs during summer and autumn in the Indian sector of the Southern Ocean, Prog. Oceanogr., 214, 103023, https://doi.org/10.1016/j.pocean.2023.103023, 2023.

Parkinson, C. L.: A 40-y record reveals gradual Antarctic sea ice increases followed by decreases at rates far exceeding the rates seen in the Arctic, Proc. Natl. Acad. Sci. U.S.A., 116(29), 14414–14423, https://doi.org/10.1073/pnas.1906556116, 2019.

Priscu, J. C., Downes, M. T., Priscu, L. R., Palmisano, A. C., and Sullivan, C. W.: Dynamics of ammonium oxidizer activity and nitrous oxide (N_2O) within and beneath Antarctic sea ice, Mar. Ecol. Prog. Ser., 62(1–2), 37–46, 1990.

Rau, G. H., Takahashi, T., Des Marais, D. J., and Sullivan, C. W.: Particulate organic matter $\delta^{13}C$ variations across the Drake Passage, J. Geophys. Res.: Oceans, 96(C8), 15131–15135, https://doi.org/10.1029/91JC01253, 1991.

Raymond, B., Meiners, K., Fowler, C. W., Pasquer, B., Williams, G. D., and Nicol, S.: Cumulative solar irradiance and potential large-scale sea ice algae distribution off east Antarctica (30°E–150°E), Polar Biol., 11, 443–452, doi:10.1007/s00300-008-0538-5, 2009.

Riedel, A., Michel, C., Gosselin, M., and LeBlanc, B.: Winter–spring dynamics in sea-ice carbon cycling in the coastal Arctic Ocean, J. Mar. Sys., 74(3-4), 918-932, https://doi.org/10.1016/j.jmarsys.2008.01.003, 2008.

Roukaerts, A., Cavagna, A. J., Fripiat, F., Lannuzel, D., Meiners, K. M., and Dehairs, F.: Sea-ice algal primary production and nitrogen uptake rates off East Antarctica, Deep-Sea Res. Part II Top. Stud. Oceanogr., 131, 140–149. https://doi.org/10.1016/J.DSR2.2015.08.007, 2016.

Roukaerts, A., Deman, F., der Linden, F. V., Carnat, G., Bratkic, A., Moreau, S., Lannuze, D., Dehairs, F., Delille, B., Tison, J.-L., and Fripiat, F.: The biogeochemical role of a microbial biofilm in sea ice: Antarctic landfast sea ice as a case study, Elem. Sci. Anthropocene, 9, 00134, https://doi.org/10.1525/elementa.2020.00134, 2021.

https://doi.org/10.5194/egusphere-2026-2645
Preprint. Discussion started: 20 May 2026

Sahashi, R., Nomura, D., Toyota, T., Tozawa, M., Ito, M., Wongpan, P., Ono, K., Simizu, D., Naoki, K., Nosaka, Y., Tamura, T., Aoki, S., and Ushio, S.: Effects of snow and remineralization processes on nutrient distributions in multi-year Antarctic landfast sea ice. J. Geophys. Res.: Oceans, 127(7), e2021JC018371, https://doi.org/10.1029/2021jc018371, 2022.

Saino, T., and Hattori, A.: ^{15}N natural abundance in oceanic suspended particulate matter, Nature, 283, 752–754. https://doi.org/10.1038/283752a0, 1980.

Schmidt, K., Atkinson, A., Stübing, D., McClelland, J. W., Montoya, J. P., and Voss, M.: Trophic relationships among Southern Ocean copepods and krill: Some uses and limitations of a stable isotope approach, Limnol. Oceanogr., 48(1), 277–289, https://doi.org/10.4319/lo.2003.48.1.0277, 2003.

Schnack-Schiel, S. B., Dieckmann, G. S., Kattner, G., and Thomas, D. N.: Copepods in summer platelet ice in the eastern Weddell Sea, Antarctica, Polar Biol., 27, 502–506, https://doi.org/10.1007/s00300-004-0613-5, 2004.

Shimada, K., Makabe, R., Takao, S., and Odate, T.: Physical and chemical oceanographic data during *Umitaka-maru* cruise of the 58th Japanese Antarctic Research Expedition in January 2017, Polar Data J., 4, 1–29, https://doi.org/10.20575/00000010, 2020.

Sommer, U., and Stabel, H. H.: Near surface nutrient and phytoplankton distribution in the Drake Passage during early December, Polar Biol., *6*(2), 107–110, https://doi.org/10.1007/BF00258261, 1986.

Sugioka, R., Matsuno, K., Takahashi, K. D., Makabe, R., Takahashi, K., Moteki, M., Odate, T., and Yamaguchi, A.: North-south changes of zooplankton community and copepods population along the 110°E line in the Indian sector of the Southern Ocean during the austral summer, Bull. Fish. Sci. Hokkaido Univ., 71(1), 39–50, https://doi.org/10.14943/bull.fish.71.1.39, 2021.

Suzuki, R., and Ishimaru, T.: An improved method for the determination of phytoplankton chlorophyll using N,N-dimethylformamide, J. Oceanogr. Soc. Japan, 46(4), 190–194, https://doi.org/10.1007/BF02125580, 1990.

Tachibana, A., Ohkubo, Y., Matsuno, K., Takahashi, K. D., Makabe, R., and Moteki, M.: Interannual and spatial variation in small zooplankton off Vincennes Bay, East Antarctica, Polar Biol., 46(9), 915–932, https://doi.org/10.1007/s00300-023-03174-0, 2023.

https://doi.org/10.5194/egusphere-2026-2645
Preprint. Discussion started: 20 May 2026

Takahashi, K. D., Makabe, R., Takao, S., Kashiwase, H., and Moteki, M.: Phytoplankton and ice-algal communities in the seasonal ice zone during January (Southern Ocean, Indian sector), J. Oceanogr., 78(5), 409–424. https://doi.org/10.1007/s10872-022-00649-2, 2022.

Takahashi, K. D., Ito, M., Sano, M., Makabe, R., Yamamoto-Kawai, M., and Ohshima, K. I.: Summer ice-algal blooms by the diatom *Fragilariopsis curta* (Van Heurck) Hustedt off Cape Darnley, Southern Ocean, Diatom, 39, 12–20, https://doi.org/10.11464/diatom.39.12, 2023.

Takahashi, K. D., Ito, M., Nojiro, N., Nomura, D., Sano, M., Aoki, S., Wongpan P., Williams G. D., Yamamoto-Kawai M., Tamura T., Moteki M., Hirawake T., and Makabe R.: Algal enrichment process for newly formed sea ice in the Dalton polynya off East Antarctica during the late summer–early autumn, Elem. Sci. Anthropocene, 13(1), 00038. https://doi.org/10.1525/elementa.2024.00038, 2025.

Takahashi, K. T., Hosie, G. W., McLeod, D. J., and Kitchener, J. A.: Surface zooplankton distribution patterns during austral summer in the Indian sector of the Southern Ocean, south of Australia, Polar Sci., 5(2), 134–145, https://doi.org/10.1016/j.polar.2011.04.003, 2011.

Thompson, P. A., and Calvert, S. E.: Carbon-isotope fractionation by a marine diatom: The influence of irradiance, daylength, pH, and nitrogen source, Limnol. Oceanogr., 39, 1835–1844, https://doi.org/10.4319/lo.1994.39.8.1835, 1994.

van der Linden, F. C., Tison, J. L., Champenois, W., Moreau, S., Carnat, G., Kotovitch, M., Fripiat, F., Deman, F., Roukaerts, A., Dehairs, F., Wauthy, S., Lourenço, A., Vivier, F,. Haskell, T., Delille, B.: Sea ice CO_2 dynamics across seasons: Impact of processes at the interfaces, J. Geophys. Res.: Oceans, 125(6). https://doi.org/10.1029/2019jc015807e2019JC015807, 2020.

Vancoppenolle, M., Madec, G., Thomas, M., and McDougall, T. J.: Thermodynamics of sea ice phase composition revisited, J. Geophys. Res.: Oceans, 124(1), 615–634, https://doi.org/10.1029/2018jc014611, 2019.

Wada, E., and Hattori, A.: Nitrogen isotope effects in the assimilation of inorganic nitrogenous compounds by marine diatoms, Geomicrobiol. J., 1(1), 85–101, https://doi.org/10.1080/01490457809377725, 1978.

Wada, E., Terazaki, M., Kabaya, Y., and Nemoto, T.: ^{15}N and ^{13}C abundances in the Antarctic Ocean with emphasis on the biogeochemical structure of the food web, Deep-Sea Res. A: Oceanogr. Res. Pap., 34(5–6), 829–841. https://doi.org/10.1016/0198-0149(87)90039-2, 1987.

https://doi.org/10.5194/egusphere-2026-2645
Preprint. Discussion started: 20 May 2026

Welschmeyer, N. A.: Fluorometric analysis of chlorophyll *a* in the presence of chlorophyll *b* and pheopigments, Limnol. Oceanogr., 39(8), 1985–1992, https://doi.org/10.4319/lo.1994.39.8.1985, 1994.

Whitaker, T. M.: Sea ice habitats of Signy Island (South Orkneys) and their primary productivity, in: Adaptations within Antarctic Ecosystems, edited by Llano, G. A., Gulf Publ., Houston, US, 75–82, 1977.

Wing, S. R., Leichter, J. J., Wing, L. C., Stokes, D., Genovese, S. J., McMullin, R. M., and Shatova, O. A.: Contribution of sea ice microbial production to Antarctic benthic communities is driven by sea ice dynamics and composition of functional guilds, Glob. Change Biol., 24(8), 3642–3653, https://doi.org/10.1111/gcb.14291, 2018.